Articles

Formation of the Rocky Mountains, Western United States: A Continuum Computer Model

PETER BIRD

One hypothesis for the formation of the Rocky Mountain structures in Late Cretaceous through Eocene time is that a plate of oceanic lithosphere was underthrust horizontally along the base of the North American lithosphere. The horizontal components of the motion of this plate are known from paleomagnetism, and the edges of the region of flat slab can be estimated from reconstructed patterns of volcanism. New techniques of finite-element modeling allow prediction of the thermal and mechanical effects of horizontal subduction on the North American plate. A model that has a realistic temperature-dependent rheology and a simple plane-layered initial condition is used to compute the consequences of horizontal underthrusting in the time interval 75 million to 30 million years before present. Successful predictions of this model include (i) the location, amount, and direction of horizontal shortening that has been inferred from Laramide structures; (ii) massive transport of lower crust from southwest to northeast; (iii) the location and timing of the subsequent extension in metamorphic core complexes and the Rio Grande rift; and (iv) the total area eventually involved in Basin-and-Range style extension.

THE FORMATION OF THE ROCKY MOUNTAINS, IN AN EVENT known as the "Laramide orogeny," has been studied by geologists for a century. It is well known that deformation began in the Late Cretaceous, peaked in the Paleocene, and waned in the Eocene. All Rocky Mountain ranges (and many smaller structures) show evidence of minor horizontal shortening of the crust in the east-west or northeast-southwest direction. This event deformed, and locally uplifted, the Precambrian metamorphic layer of the crust (known as "basement") as well as the thin veneer of Paleozoic and Mesozoic sedimentary rocks. Although there has been much controversy (*1*) over the exact mechanism of basement uplifts, nearly all workers would agree that the total shortening of the upper crust in Wyoming was roughly 5% (*2*) to 10% (*3*). This shortening is not enough to explain the thickening of the crust from about 33 to over 55 km that also occurred during the Laramide orogeny (*4*); this thickened crust now isostatically supports the high regional elevation. Thickening of the crust by igneous intrusions during the orogeny was three orders of magnitude too small to explain this increase, even if generous assumptions are made about the size of intrusive bodies at depth (*4*). Therefore, some mechanism that involves large strains in the ductile lower crust must be inferred. One additional complication is that most of the Laramide basement uplifts were covered by sedimentary rocks soon after their formation, only rising to become topographic features after the end of Laramide time (*5*).

The concept that the Rockies might have been formed by "subcrustal convection currents" goes back at least to Longwell (*6*), who applied concepts of Holmes and Griggs to this region. These

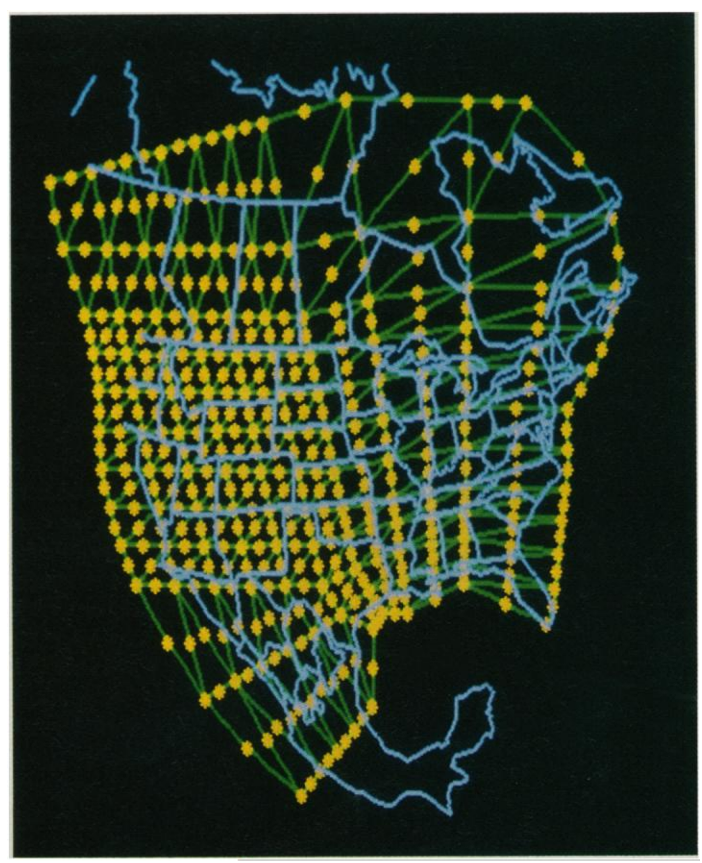

Fig. 1. Grid of finite elements that was used to represent the crust of North America. An identical second grid underneath is used to represent the mantle layer of the lithosphere. Each layer is composed of 437 nodes (yellow) and 198 isoparametric triangles (green), within which quadratic functions are used to represent velocity and layer thickness. Each triangle contains seven integration points (not shown) for all area and volume integrals. In this and other figures, the West Coast is omitted from the base map of state lines (blue) because its past configuration is controversial.

The author is professor of geophysics in the Department of Earth and Space Sciences, University of California, Los Angeles, CA 90024.

Fig. 2. Areas of flat subduction at various times in the past. The labeled curves separate the area that was underlain by flat-subducting oceanic slabs (to the west) from areas that were underlain by normal asthenosphere (to the east). Thus, these lines are the locations at which the oceanic plates separated from North America and descended into the asthenosphere. Curves are labeled in millions of years before present. For more complete data and maps see (*4*).

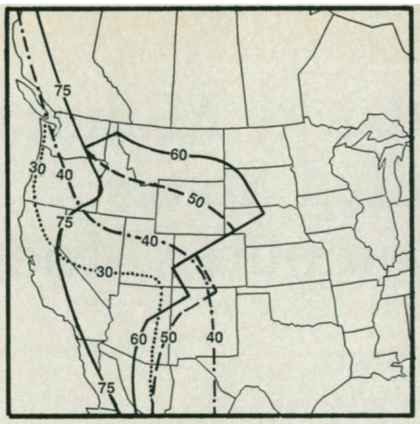

early writers conceived of the crust (the surficial layer of more silicic composition) as rigid-plastic, and the mantle as a uniformly fluid layer of no long-term strength ("asthenosphere"). It is now postulated that the top of the mantle also contains a cold, rigid thermal boundary layer (the "mantle lithosphere") that overlies the asthenosphere. Paleomagnetic data also indicate conclusively that vast areas of oceanic crust and attached lithosphere were subducted (underthrust) beneath the west coast of North America during the time of the Laramide orogeny (*7, 8*). A link between subduction and the orogeny was suggested by Dickinson and Snyder (*9*), who proposed that the subduction was horizontal, with the oceanic lithosphere sliding along the base of North America as far inland as the Black Hills. They suggested that the resulting shear stresses caused the shortening strains seen at the surface. Horizontal subduction has also been invoked to explain the sudden subsidence of the region in the Late Cretaceous (*10*). Finally, I have previously suggested (*4*) that horizontal subduction transferred crustal material into the Rockies region from the southwest, which increased the crustal thickness by about 65%.

In this article I present a test of the hypothesis of flat subduction by a quantitative prediction of its effects. This has been done with a set of new finite-element techniques developed especially for this problem (*11*) that permit the calculation of crust and mantle-lithosphere displacement, thickness, and temperature through time. The boundary conditions of the simulation are obtained from plate tectonic theory and are reasonably certain.

This model does not have the spatial resolution to predict individual structures such as the Wind River or Big Horn ranges, but it does consistently predict a curved belt of crustal compression with the correct location, timing, and orientation. (However, the amplitude is adjustable, because it depends on the assumed rheology.) Furthermore, the model predicts the transfer of lower crustal material into the Rockies region from the coastal region in a great wave. After the eventual removal of anomalous masses in the mantle, this extra crust would cause a buoyant uplift, which explains the present elevations. Another, unexpected feature of these solutions is that the mantle layer of the North American lithosphere is entirely stripped away from the region west of the Rockies. This provides a simple unifying explanation for the cause, location, and timing of the extensional strain event ("taphrogeny") that followed the Laramide orogeny and created the Basin-and-Range topography. Thus, the hypothesis of horizontal subduction both provides a fundamental mechanism for the Laramide orogeny and suggests an explanation for the next event, which until recently was considered distinct and unrelated.

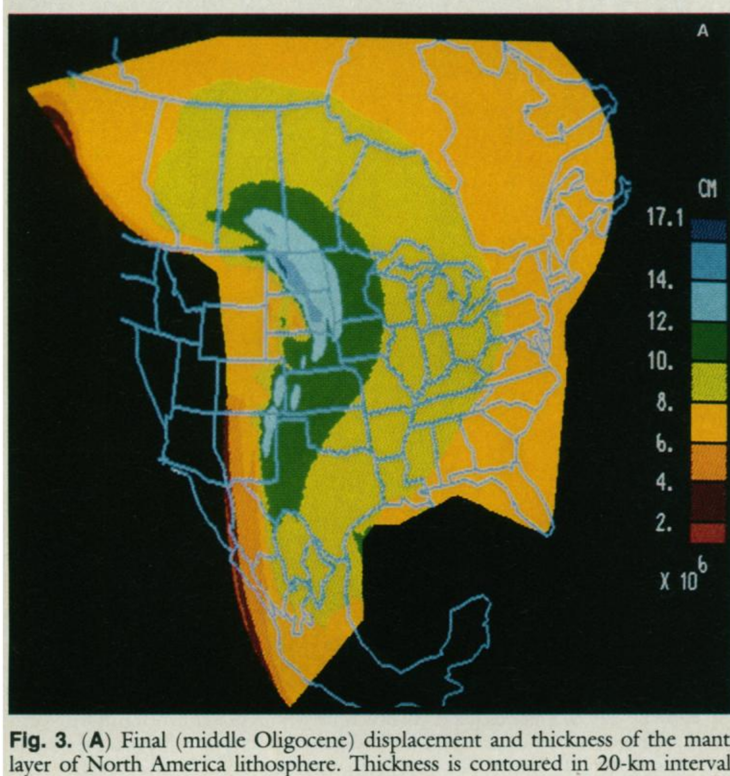

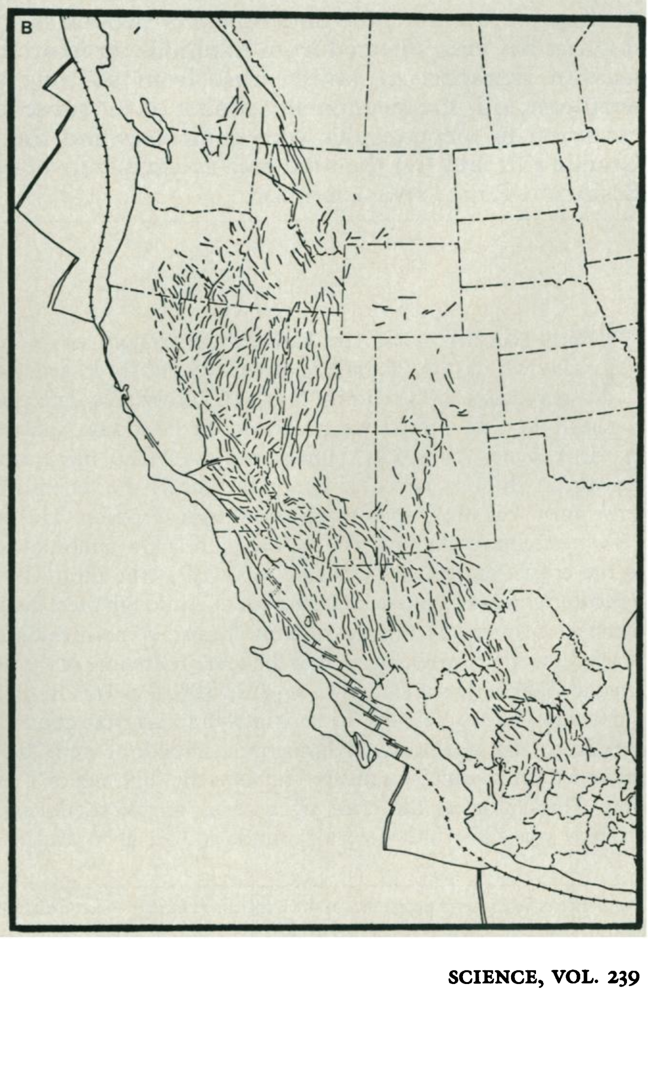

Fig. 3. (**A**) Final (middle Oligocene) displacement and thickness of the mantle layer of North America lithosphere. Thickness is contoured in 20-km intervals. (**B**) Summary map of post-Oligocene faults in North America, from Stewart (*33*). Most (except the San Andreas fault system) were formed in the extensional Basin-and-Range taphrogeny that continued after the end of this model. Note the correspondence between the area that was cleared of mantle lithosphere and the area that was eventually extended.

Computational Methods

The simulation problem is an initial-value problem in the Stokes–creeping-flow equation, linked with the heat-diffusion equation, and subject to a mixture of velocity and stress boundary conditions. The complete derivation of the model equations is given in (*11*). The calculation is difficult because the strength of rocks is exponentially dependent on temperature (above some transition temperature), and temperature gradients are large and depend on the deformation. The duration of this model (45 million years) is such that neither an adiabatic nor a steady-state approximation of temperatures is adequate. Thus, the calculation proceeds through time steps of 1 million years, each of which is artificially partitioned into an adiabatic translation and a static period of heat diffusion.

The model domain is the lithosphere of North America, which is very much wider (5000 km) than it is thick (100 km). Therefore, it is adequate to solve the Stokes equation in vertically integrated form, which effectively condenses the strength of the lithosphere into a single plane. The horizontal components of velocity are then computed by the "thin-plate" finite-element method (*12–14*). In this approach, two-dimensional finite-element grids are used to represent the strong crust and mantle lithosphere layers, but their assigned properties reflect the results of three-dimensional volume integrals throughout the layers. This method reduces the finite-element grid from three dimensions to two (Fig. 1), with an indispensable reduction in cost. Vertical force equilibrium is represented by the isostatic approximation; each column floats on a fluid support at an elevation determined by its density structure. Time integrations are performed by the predictor-corrector scheme. The finite-element grid deforms over time to follow the path of the more rigid material at the top of each layer.

One innovation in this project is the use of two stacked grids (initially identical) to represent the crust and mantle layers of the North American lithosphere, respectively; this allows their velocities to differ, which is an essential feature of the model. The vertical integration of strengths is performed numerically at each of seven integration points in each finite element. A simultaneous vertical integration of compliance (inverse of effective viscosity) provides the coefficients that are necessary to compute the shear stresses between the layers when their horizontal velocities differ.

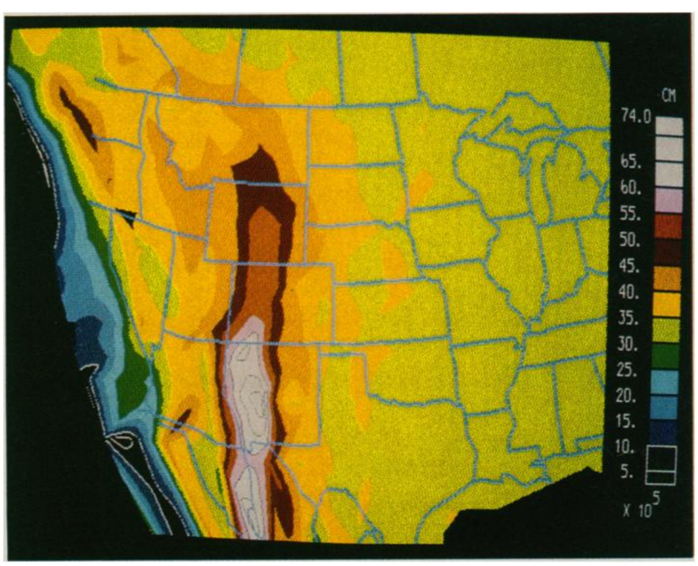

Fig. 4. Final (middle Oligocene) predicted crustal thickness. Contour interval is 5 km. Crust has been transported by simple shear from the coastal region, where it was thinned, to the longitude of the Rockies, where it was thickened. This thickening isostatically supports the present regional elevation (up to 2 km) of the Rockies. Thickening in the Great Plains was actually greater than in this model. Final thicknesses near the coast are too small because coastal cordillera was omitted from the initial condition. Extreme thicknesses shown in New Mexico are not present today but may have been attenuated by extension in the Rio Grande rift.

The rate of thickening of each layer is determined by the incompressibility condition, which is applicable exactly to anelastic strains. Like displacement, layer thickness is assumed to be laterally continuous and is parameterized by quadratic finite-element basis functions.

One effect that causes thickness changes is divergence, in the horizontal plane, of the horizontal velocity of the grid that represents the strong upper part of each layer. This will be referred to as "pure shear" because it is irrotational in any vertical cross section. A second effect is divergence, in the horizontal plane, of the flux of ductile material that is involved in "simple shear" to accommodate different horizontal velocities of layers. This flux depends on the difference between the horizontal velocities of the grids and on the vertical temperature gradient, which determines the thickness of the simple-shear boundary layer. Wherever crust is transported by simple shear, it is assumed to remain part of the crustal layer and not to be dragged down below mantle material; in nature this would be enforced by compositional density contrasts—unless a part of the lower crust with gabbroic composition underwent a phase change to dense eclogite. A third effect is independent flow of ductile material in response to lateral pressure gradients associated with topography ("gravity spreading"). In the crust, this effect tends to smooth the thickness through a nonlinear "diffusion" of crustal thickness (*15*). Effects of erosion and deposition on crustal thickness are neglected.

In the computation of temperatures, lateral heat conduction is neglected. At each of the seven integration points of each of the elements, the geotherm (temperature as a function of depth) is represented as the sum of steady-state quadratic functions and a set of five decaying eigenfunctions of the homogeneous one-dimensional diffusion equation. Wherever simple shear between layers would tend to cause a temperature discontinuity at the base of a layer, an appropriate z^3 term is added to the geotherm (where z is depth).

Convergence tests documented in (*11*) suggest that the results presented in this article have a relative precision (root-mean-square error/root-mean-square signal) of about 15% for the variables of crust and mantle displacement and mantle thickness. However, the changes in crustal thickness have only about 50% root-mean-square relative precision and should be considered as suggestive rather than definitive. Greater precision is not presently attainable, as each run already consumes about 2 hours on either a Cray X-MP/48 (1 processor) or an IBM 3090/VF. The main reason for this expense is that the nonlinearity of the rheology requires about 14 iterations of the velocity solution per time step.

Rheology of North America

In these calculations the total strains of interest range from 0.05 up to 1000; therefore, the contribution of elastic strain is negligible. Deformation is governed by one of three laws based on laboratory experiments, each of which places an upper limit on the shear stress, σ_s. Each law is written for an isotropic material, partly for simplicity and partly out of ignorance. At low temperature, the important limit is set by frictional sliding on any and all planes:

$$\sigma_s \leq \mu(\sigma_n - P_{H_2O}) \qquad (1)$$

where μ is the coefficient of friction, σ_n is the (positive) normal stress on the same plane, and P_{H_2O} is the pressure of water in pores (assumed hydrostatic). At higher temperatures, the relevant limit is set by thermally activated, power-law dislocation creep:

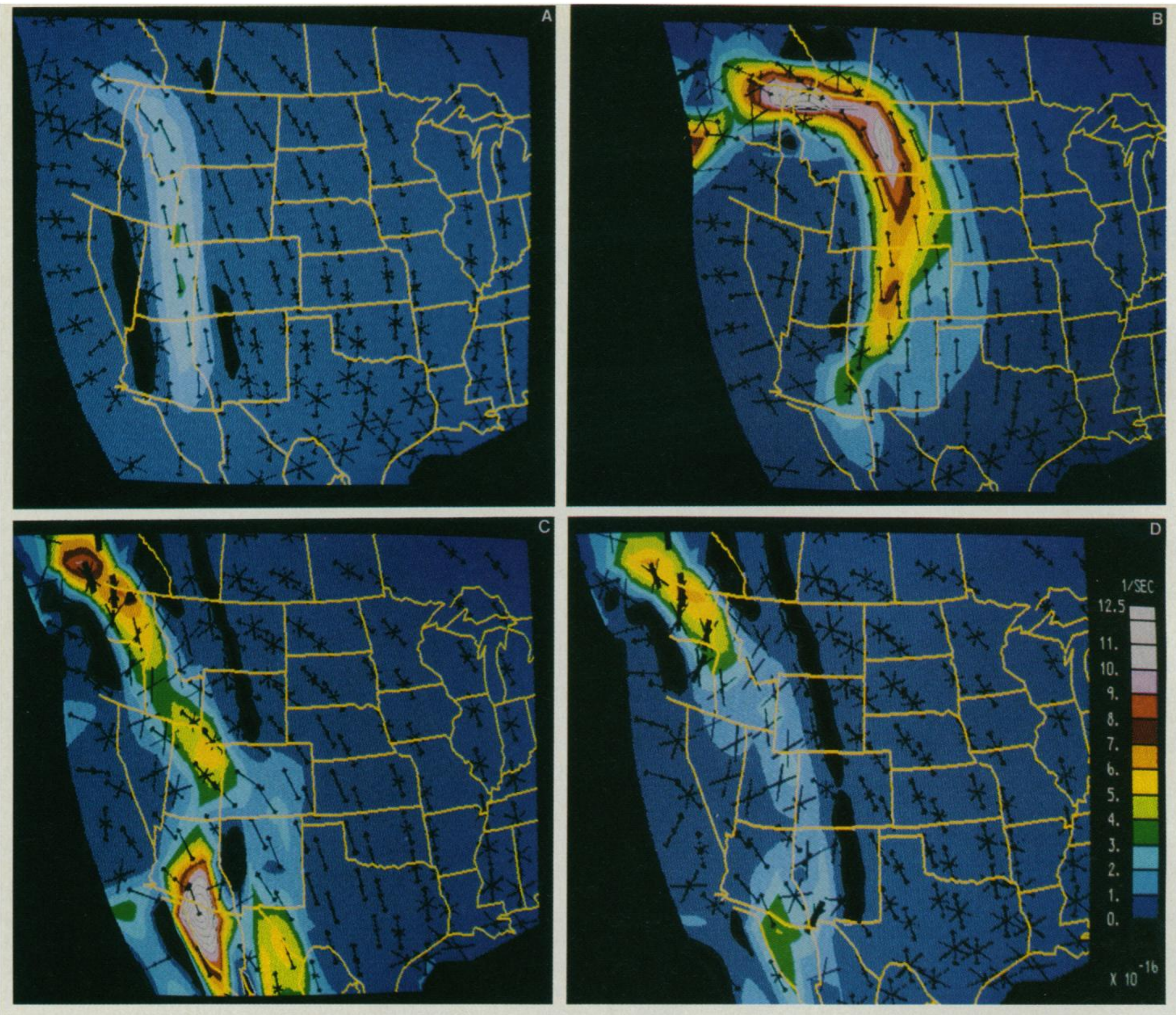

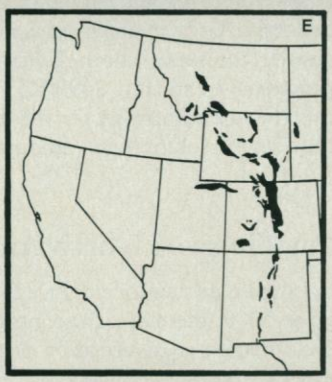

Fig. 5. Maps of strain rates (shown by color code) and strain type (shown by fault symbols) at the surface at four important times in the model. Color contour interval is 10^{-16} per second. Black symbols show representative fault trends: X pattern shows conjugate strike-slip faults; baton pattern shows strike of thrust faults; rectangle (representing a graben) shows strike of normal faults. A strike-slip component is commonly superposed on either thrust faulting (shortening) or normal faulting (extension). (**A**) Sixty-nine million years ago (latest Cretaceous); (**B**) 64 million years ago (early Paleocene); (**C**) 39 million years ago (late Eocene); (**D**) 34 million years ago (early Oligocene; (**E**) present pattern of Laramide basement uplifts (black) for comparison with (B).

$$\sigma_s \leq 2\alpha[2(-\dot{e}_1\dot{e}_2 - \dot{e}_2\dot{e}_3 - \dot{e}_3\dot{e}_1)^{1/2}]^{(1-n)/n}\dot{e}_s \exp\left(\frac{\beta + \varepsilon P}{T}\right) \quad (2)$$

where $\dot{e}_i$ are the principal strain rates, $\dot{e}_s$ is the shear strain rate (on the same plane as σ_s), P is total pressure, T is absolute temperature, and α, β, ε, and n are empirical constants. (Values of these and other parameters are contained in Table 1.) The third limit is a plasticity condition which is independent of P and T:

$$\sigma_s \leq \sigma_p \quad (3)$$

In applying all of these laws, the vertical stress σ_{zz} is assumed to be lithostatic. To avoid numerical difficulties, an upper limit, η_{max}, is also placed on the effective viscosity at all points.

It should be noted that two of these parameters (α and β of the crust) were adjusted to values that give the proper magnitude of Laramide surface strain. However, these values have to be taken in the context of many other assumed parameter values (especially thermal parameters) and are not presented as experimental determinations.

Initial Conditions

The model begins 75 million years ago, in the Late Cretaceous. At that time, the future Rocky Mountain region and Great Plains were close to sea level and had been since the late Cambrian (*16*). A region from eastern Utah to the Texas panhandle was deformed in the late Paleozoic Ancestral Rockies orogeny, but this topography had been completely eroded by Laramide time. Therefore, I assume that heat diffusion had established a uniform steady-state geotherm with a typical platform heat flow of 54 mW m^{-2}, and that the combination of isostasy, erosion, and deposition had leveled the crust to a uniform thickness of 33 km. The initial thickness of 70 km that was chosen for the mantle lithosphere is somewhat arbitrary because the lithosphere-asthenosphere boundary is gradational. Because the strength of the mantle lithosphere is concentrated at its top, the lower limit of integration makes little difference.

Much has been written about the probable influence of earlier structures (such as the Ancestral Rockies) on Laramide deformation. Unfortunately, such structures cannot be included in the model. There is a problem of resolution, and a more significant problem that the structures are only known where Laramide uplifts have caused sufficient erosion to strip off the sedimentary rock cover and expose them. To include these, while omitting all buried structures, would unacceptably bias the results. Instead, we need to determine first how much geologic history can be understood through continuum models before adding such complications.

Further west, within about 600 km of the coast, there was a mountain belt comparable to the present Andes (*17*). This belt had developed during the previous 80 million years above a subduction zone of typical geometry, and its eastward spreading under the force of gravity may have been responsible for the Cretaceous Sevier orogeny that formed the Overthrust Belt (*17*). Initially, I attempted to include such a belt of thickened crust and high topography (cordillera) in the initial condition. But it was soon apparent that the balance of forces in such a system is subtle and not easily guessed, for I could not find an initial condition that would be in quasi–steady state along its whole length simultaneously. This level of realism is deferred to future studies, and the reader is cautioned that crustal thicknesses were originally greater to the west of the Rockies than in the model that is presented.

Boundary Conditions

The northern, eastern, and southern margins of the finite-element grid (Fig. 1) are fixed. Boundaries in Mexico and Canada are placed where Laramide strain becomes secondary to the effects of other Tertiary orogenies that are not modeled—those in the Caribbean and in Alaska. The eastern and Gulf coast boundaries are natural; the strength of oceanic lithosphere is so much greater than that of the continental lithosphere that strain is negligible in the former. The western edge of the continent was the upper plate of a subduction zone, so this edge was tapered and does not require a boundary condition.

The bottom boundary is divided into two areas: the area overlying normal hot asthenosphere and the area overlying flat-subducting oceanic plate. The boundary between these areas moved inland and then westward again during the modeled interval (Fig. 2), and its progress may be tracked by the changing patterns of volcanism in the western United States (*4, 9*).

Where mantle lithosphere overlies asthenosphere, the temperature at the base of the lithosphere is fixed (by convection) at 1440 K. However, where asthenosphere comes into contact with the crust, I assume that crustal melting or convection will limit the temperature at the base of the crust to 1073 K. Mechanically, asthenosphere is a perfect fluid (with density 3210 kg m^{-3}) in which there are no shear stresses.

To determine the excess mass of the oceanic slab (with respect to the asthenosphere it displaces), I first reconstruct the Farallon plate of oceanic lithosphere, using finite rotations from Engebretson *et al.* (*8*). I then apply the boundary-layer cooling model by assuming that the vertically integrated excess weight of the oceanic slab with respect to asthenosphere is 6600 Pa $\times$ $t^{1/2}$, where t is the age of the slab (cooling time) in years. The normal fluid support pressure on the bottom boundary is reduced by this amount; therefore, after isostatic adjustment, the surface of the continent is depressed by about 2 to 3 km above the slab (*4, 10*). The horizontal velocities of the slab are obtained from rotation poles of Engebretson *et al.* (*8*), and used as velocity boundary conditions on the contacted area. Note that velocity is imposed on the weak base of the bottom layer, and the velocity of the strong upper levels and its finite-element grid may be less, depending on rheology and temperature. Also, the shear stress that is necessary to impose this velocity boundary condition is monitored, and, if it exceeds 100 MPa, then that shear stress is substituted (to simulate formation of a ductile fault). The appropriate value of this stress limit is the most uncertain of the model parameters (*18*).

Where this slab makes contact with the base of North America, a temperature boundary condition of 700 K is imposed. This value is the average obtained in a two-dimensional finite-difference model of heat advection and diffusion (including the oceanic plate in the domain) that was conducted separately for a representative cross section. Of course, a more realistic boundary condition would be needed before final estimates of the optimal plate rheology can be determined. (A new version of the model is being developed in which the temperature calculations encompass either the slab or the asthenosphere or both below North America.) Note that the imposed boundary temperature is lower than the initial temperature at the base of either crust or mantle lithosphere; therefore, the thermal effect of the slab is to cool and strengthen the parts of the continent that it touches.

Summary of the Model

As the flat-subducting slab of oceanic lithosphere began to slide along the base of North America, it initially contacted the base of the mantle lithosphere at about 100-km depth. The cold slab chilled and strengthened this mantle lithosphere, which originally lay along the coast, forming a "mantle plate" that subsequently moved northeast without internal deformation or thickening (Fig. 3); deformation occurred in the mantle lithosphere that was farther inland and had not yet been chilled. Although the shear stress applied to this strong edge was limited, the cumulative force set the entire mantle lithosphere of North America in motion to the northeast (with respect to the crust), at various fractions of the velocity of the Farallon plate (which moved at up to 12 cm $year^{-1}$). The mantle lithosphere moved without displacing the upper crust, from which it was detached by a weak shear zone in the lower crust. The mantle lithosphere was shortened horizontally and thickened vertically by pure-shear strain, and was left beneath the Great Plains and central lowlands.

After the mantle lithosphere was removed, the oceanic plate dragged directly on the crust. The crust was chilled and strengthened, but because of its lower creep-softening temperatures, it did not become rigid. Rather, a simple-shear zone in the lower crust accommodated the relative velocity over a huge area. Since the scale thickness of this shear zone was only 2 to 3 km and the relative displacement was of order 3000 km, shear strains of order 1000 accumulated in the lower crust. A thin boundary layer of crust was transported with the oceanic plate, which caused crustal thinning in the west and crustal thickening in the east (Fig. 4). This crustal thickening in the Rockies gradually reversed the initial subsidence that had been caused by the weight of the slab.

These basal tractions generated horizontal compressive stress at the surface, as suggested by Dickinson and Snyder (*9*). This stress was largest at the northeastern margin of the region of flat subduction, as required by the stress equilibrium equation. In addition, this relatively depressed region had less vertical topographic stress to resist shortening. This is why surface shortening strains form an arc from Montana to New Mexico in all models, regardless of rheological parameters. (In this particular model, the average net strain in Wyoming has been adjusted to 11% shortening by experimenting with the crustal rheology.) The maximum strain rates at the surface occurred when the flat slab area reached maximum width in the early Paleocene (Fig. 2).

Later, the region of flat subduction contracted, and the inland volcanic arc returned westward toward the coast. Paleomagnetic data rule out any reversal of oceanic-plate motion, so we must infer that the hinge line that terminates the flat-slab area moved west while the slab continued to move east. (There is no particular dynamical difficulty in this because hingelines are always moving in the reference frame of the slab.) Consistent with the continuum approach, I assume that the oceanic slab peeled away and sank as a continuous sheet without leaving any fragments attached to North America.

Westward migration of the hingeline exposed the base of the crust to upwelling hot asthenosphere over a vast region west of the Rockies (Fig. 3). Heating from below decreased the strength of the crust progressively over about 10 million years (*19*), while isostatic rebound increased its elevation and therefore the tendency for gravitational spreading. Thus, crustal extension followed several million years after the removal of the flat slab, but only in the region from which the mantle lithosphere had been removed. Extension was simultaneous with flat subduction farther west; compressive stresses that were caused by flat subduction were insufficient to overcome the spreading tendency of the thickened, heated, and uplifted crust.

Comparison to Geologic History

The prediction of vertical crustal movements is the least successful part of the model. The Rocky Mountain foreland region actually (i) subsided by as much as 3 km sometime between 84 million and 66 million years ago (*10, 16*); (ii) rose past sea level slightly before 65 million years ago, stopping at perhaps 1 km (*5*); and (iii) acquired its present 2-km elevation after 30 million years ago, perhaps in the Pliocene (*5*). The model shows a similar pattern, but with offsets in the timing. The surface is (i) depressed to −4.5 km at about 67 million years ago, when the flat slab and the thickened North American lithosphere underthrust the crust; (ii) uplifted to sea level [which meanwhile had dropped 100 to 200 m (*20*)] during 66 million to 55 million years ago by a combination of pure shear, arrival of imported crust, and retreat of the flat slab; and (iii) left at about 1 km when the model ends 30 million years ago. If we assume that the overthickened mantle lithosphere was later removed by convection (*21*) or delamination (*22*), then the model would be consistent with a second, late uplift to 1.5 km or 2.5 km, respectively. Thus, the most important discrepancy is that events are about 10 million years late in the model.

It is likely that some of this error is inherited from incorrect assumed positions of the flat part of the oceanic plate that were used in the bottom boundary condition. As detailed in (*4*), the boundary condition that I assumed was a northeastward intrusion of a flat slab such that intrusion begins at 75 million years ago and the flat slab reaches the Rocky Mountain region about 10 million years later. If we accept the suggestion of Cross (*10*) that the coastal volcanic arc lost its heat source when magmatism began to wane near the coast 80 million years ago, then the whole history of flat subduction could be advanced 5 million years, which halves the discrepancy. Furthermore, if the oceanic plate, which was already dipping beneath the Rocky Mountain region, decreased its angle of dip uniformly, it might have contacted a large area of North America simultaneously, without a 10-million-year delay. Thus, it seems possible within the constraints of the data to advance many of the model events by up to 15 million years.

The predicted final crustal thickness that is shown in Fig. 4 also has important defects. The long north-south belt of very thick (over 55 km) crust is predicted to fall along 106°W, whereas present seismic refraction data place it farther east, near 100°W. It seems that the present model gives an insufficient amount of transport of crust above the displaced North American mantle lithosphere; this might be remedied in future models that have a more realistic crustal structure with layered creep properties. The large thicknesses that were predicted to occur in New Mexico are certainly not evident today, but this does not necessarily mean that the model is wrong; late Tertiary extension of the Rio Grande rift may have been driven by gravitational spreading of this crustal root, which would diminish its amplitude. The essential point about crustal thickness is that only models of this tectonic style are capable of predicting inland crustal thickening far greater than that attributable to horizontal shortening of the upper crust (*4*).

The predicted Oligocene thickness of the mantle lithosphere (Fig. 3) is the most difficult result to test, as even the present thickness is uncertain. Also, some of this dense mantle may have been removed convectively; it is actually necessary to assume this in order to explain the late Tertiary uplift of the Great Plains to their present height (*5*). It is worth noting, however, that thickened mantle lithosphere provides an explanation for the anomalously high seismic velocities that are inferred in the upper mantle of the midcontinent (*23*).

The model's best feature is its prediction of the history of surface strain (Fig. 5). During 70 million to 65 million years ago (latest Cretaceous), it predicts a belt of slow shortening that extends from

Table 1. Parameters of the North American plate.

Parameter	Symbol	Crust	Mantle	Units	Ref.
Friction coefficient	μ	0.85	0.85		(*32*)
Viscosity factor	α	172	6,390	Pa $sec^{1/n}$	
(Activation energy)/nR*	β	14,000	18,300	K	
Stress exponent	n	3.0	3.5		(*32*)
(Activation volume)/nR*	ϵ	0.	5.8×10^{-7}	K Pa^{-1}	(*32*)
Plasticity stress	σ_p	5×10^8	5×10^8	Pa	(*32*)
Maximum viscosity	η_{max}	3×10^{24}	3×10^{24}	Pa sec	
Initial thickness		3.3×10^4	7×10^4	m	
Radioactive heating		6.1×10^{-7}	1.6×10^{-8}	J m^{-3} sec^{-1}	
Thermal conductivity		2.5	4.06	J m^{-1} sec^{-1} K^{-1}	
Thermal diffusivity		1.2×10^{-6}	1.2×10^{-6}	m^2 sec^{-1}	
Initial heat flow at top		0.054	0.034	J m^{-2} sec^{-1}	
Density at STP†		2,988	3,248	kg m^{-3}	

*R is the ideal gas constant. †Standard temperature and pressure.

western Montana south through Utah to eastern Arizona. This corresponds nicely to some of the more western Laramide structures: the Blacktail-Snowcrest and Madison ranges in Montana were formed in the latest Cretaceous (*24, 25*), and thrust faulting in southern Arizona is also partly Cretaceous in age (*26*). The central part of this belt overlaps the preexisting Overthrust Belt from the waning Sevier orogeny, which in fact experienced its last major shortening about 70 million years ago (*27*).

The region of maximum predicted shortening then moves eastward to a long arc in Montana–Wyoming–Colorado–New Mexico and remains there from 64 million to 45 million years ago (early Paleocene through middle Eocene) with waning intensity. As shown in Fig. 5, there is a striking resemblance between the predicted region of maximum strain and the location of the well-known belt of Laramide basement uplifts in these states; furthermore, the predicted orientations of thrust faults coincide with the long axes of the uplifts and many observed thrust fault trends. The predicted ages of many uplifts are correct, although some are predicted up to 10 million years late (*28*). Paleocene crustal shortening that actually occurred in British Columbia is not predicted, but this can be excused as a consequence of omitting the coastal cordillera from the initial condition, as discussed above.

The last phase of compression around 40 million years ago is displaced to the southwest into northern Utah, and the axis of shortening is rotated counterclockwise to N35E. This new direction should be compared to the late formation of the Uinta Range at an anomalous trend to other Laramide structures (*28*). The range actually runs more nearly east-west, not west-northwest to east-southeast as predicted, but it is widely believed that its trend was controlled by Precambrian rift structures. Also, the range formed in middle Eocene time, so once again the model is late by 4 million to 12 million years.

The model predicts no later compression, except in southern Arizona. Meanwhile, an area of crustal extension begins to expand at 46 million years and spreads from southern British Columbia southeast into Washington and Oregon by 40 million years ago, into Montana-Idaho by 35 million years ago, and into southwestern Wyoming by 30 million years ago. A second region of extension appears in southern New Mexico at 35 million years ago. The northern region of extension is triggered by heating and uplift of the crust exposed to the asthenosphere; the southern region is driven by gravity spreading of very thick crust (Fig. 4).

This extensional phase is the beginning of the Basin-and-Range taphrogeny. In the north, it was expressed by formation of "metamorphic core complexes" with low-angle normal faults in Washington about 51 million years ago (*29*) and along the Montana-Idaho border about 45 million to 40 million years ago (*30*). Once again, the model gives the correct pattern, but is 5 million to 10 million years late. In the south, extension was expressed by initial formation of the Rio Grande rift 32 million years ago (*31*); the model is correct here.

The model ends 30 million years ago because it is not yet equipped to model the contact of North America with the Pacific plate and formation of the San Andreas fault system. However, the Basin-and-Range taphrogeny continued and expanded up to the present day. In advance of further calculations, it is safe to predict that some degree of extension will affect all areas of the models that lose their mantle lithosphere and are therefore eventually exposed to hot asthenosphere. Figure 3 shows that there is a remarkable agreement between the area that was swept free of subcrustal lithosphere and the area that was subsequently involved in late Tertiary faulting (except the Rio Grande rift, which had a different mechanism). This suggests that removal of lithosphere by horizontal subduction is the key factor that controls the extent and timing of the Basin-and-Range taphrogeny.

Conclusions

In a broad sense, this model has predicted the belt of Laramide structures, the transport of crust from the coastal region to the continental interior, the subsequent extension in metamorphic core complexes and the Rio Grande rift, and the geographic region of late Tertiary Basin-and-Range extension. Its principal defects are that (i) many events are predicted about 5 million to 10 million years too late and (ii) the wave of crustal thickening does not travel far enough to the east. Reasonable modifications to the oceanic plate kinematics and rheologies that were assumed may correct these defects.

The correspondence of model predictions to actual geology is already sufficiently close to show that the hypothesis that horizontal subduction caused the Laramide orogeny is probably correct. The Rocky Mountain thrust and reverse faults formed in an environment of east-west to northeast-southwest compressive stress that was caused by the viscous coupling between the oceanic plate and the base of the North American crust. Nonuniform crustal thickening by simple-shear transport also caused relative uplifts; therefore, this model is consistent with both of the range-forming mechanisms that have been inferred (*1*). A new proposal that arises from this simulation is that horizontal subduction also caused the subsequent extensional Basin-and-Range taphrogeny by stripping away the mantle lithosphere so that the crust was exposed to hot asthenosphere after the oceanic slab dropped away.

REFERENCES AND NOTES

1. G. D. Couples and D. R. Lageson, *Geology* **13**, 311 (1985).
2. G. D. Couples and D. W. Stearns, *Geol. Soc. Am. Mem.* **151**, 313 (1978).
3. R. Gries, *Am. Assoc. Pet. Geol. Bull.* 67, 1 (1983).
4. P. Bird, *Tectonics* **3**, 741 (1984).
5. D. E. Trimble, *Mt. Geol.* 17, 59 (1980).
6. C. R. Longwell, *Am. J. Sci.* **243A**, 417 (1945).
7. T. Atwater, *Geol. Soc. Am. Bull.* **81**, 3513 (1970).
8. D. C. Engebretson, A. Cox, R. G. Gordon, *Geol. Soc. Am. Spec. Pap.* **206**, 1 (1985).
9. W. R. Dickinson and W. S. Snyder, *Geol. Soc. Am. Mem.* **151**, 355 (1978).
10. T. A. Cross and R. H. Pilger, *Nature (London)* **274**, 653 (1978); T. A. Cross, *Spec. Publ. Int. Assoc. Sedimentol.* **8**, 15 (1986).
11. P. Bird, in preparation.
12. ______ and K. Piper, *Phys. Earth Planet. Inter.* **21**, 158 (1980).
13. J. P. Vilotte, M. Daignieres, R. Madariaga, *J. Geophys. Res.* **87**, 10709 (1982).
14. P. C. England and G. A. Houseman, *Nature (London)* **315**, 297 (1985).
15. P. Bird and D. V. Kemp, *Eos* **68**, 1465 (1987) (abstr.).
16. W. W. Mallory, Ed., *Geologic Atlas of the Rocky Mountain Region* (Rocky Mountain Association of Geologists, Denver, 1972).
17. B. C. Burchfiel and G. A. Davis, *Am. J. Sci.* **275A**, 363 (1975).
18. It would be best to determine this stress limit from the rheology of subducted sea floor sediment, but too little is known about its composition, porosity, and pore pressure under these conditions. Those who believe in "passive mantle convection," whereby the density anomalies in plates drive the flow, will find 100 MPa unacceptably high. Therefore, this model in its present form is only tenable if there is (sometimes) "active mantle convection," with plates driven from below.
19. P. Bird, *J. Geophys. Res.* **84**, 7561 (1979).
20. P. R. Vail, R. M. Mitchum, Jr., S. Thompson III, *Am. Assoc. Pet. Geol. Mem.* **26**, 83 (1977).
21. G. A. Houseman, D. P. McKenzie, P. Molnar, *J. Geophys. Res.* **86**, 6115 (1981).
22. P. Bird and J. Baumgardner, *ibid.*, p. 4891.
23. J. Cleary and A. L. Hales, *Bull. Seismol. Soc. Am.* **56**, 467 (1966); A. L. Hales and J. L. Roberts, *ibid.* **60**, 461 (1970).
24. D. J. Nichols, W. J. Perry, Jr., J. C. Haley, *Geology* **13**, 149 (1985).
25. R. G. Tysdal, R. F. Marvin, E. DeWitt, *Geol. Soc. Am. Bull.* **97**, 859 (1986).
26. G. B. Haxel, R. M. Tosdal, D. J. May, J. E. Wright, *ibid.* **95**, 631 (1984).
27. R. L. Armstrong, *ibid.* 79, 429 (1968).
28. R. Gries, in *Rocky Mountain Foreland Basins and Uplifts*, J. D. Lowell and R. Gries, Eds. (Rocky Mountain Association of Geologists, Denver, 1983), p. 9.
29. D. Parkinson, *Geol. Soc. Am. Abstr. Prog.* 17, 399 (abstr.) (1985).
30. D. W. Hyndman, *Terra Cognita* 7, 59 (abstr.) (1987).
31. M. J. Aldrich, Jr., C. E. Chapin, A. W. Laughlin, *J. Geophys. Res.* **91**, 6199 (1986).
32. S. H. Kirby, *Rev. Geophys. Space Phys.* **21**, 1458 (1983).
33. J. H. Stewart, *Geol. Soc. Am. Mem.* **152**, 1 (1978).

34. This work was supported by the National Science Foundation through grant EAR 85-07665 to the University of California. Computing support in the form of matching time on the IBM 3090/VF was also provided by the University of California, Los Angeles, through its Office of Academic Computing.